MANSOURA JOURNAL OF CHEMISTRY
Official Journal of Faculty of Science, Mansoura University, Egypt
E-mail: scimag@mans.edu.eg ISSN: 2974-4938

Graphene supported MIL-125 Polyurethane foam for Solar Water Desalination

O. R. Hayes, S.E. Samra, Awad I. Ahmed *

Chemistry Department, Faculty of Science, Mansoura University, Al-Mansoura 35516, Egypt.

**Corresponding author at, Chemistry Department, Faculty of Science, Mansoura University, Mansoura, Egypt.*

Received:12/4/2023
Accepted: 26/4/2023

Abstract: seawater desalination is an important strategy to give clean sources for water treatment by solar evaporators to produce heat from the solar in recent years. Herein, for solar steam generation, we prepare MIL-125 mixed with polyurethane foam (MPU). We improved MPU by using graphene oxide to enhance the evaporation rate. Polyurethane foam has various advantage such as floating property and self-pump water by its hydrophilic structure The porosity property of the fabricated polyurethane foam was noticed in the SEM images which include the hydrophilic nature and the open porous of the fabricated Polyurethane foam. MIL-125 has large salt rejection, and large water permeability. GO enhanced solar absorption, and photo-thermal conversion efficiency since it exhibits broad band light for steam generation uses. Under one solar irradiation, the mass change of water by GO@MIL-125 (MG) nanocomposite (0.62 kg m^{-2}) is larger than MIL-125 (0.44 kg m^{-2}) (M). Additionally, the evaporators exhibit organic dye removal from contaminated water and produces pure condensed freshwater.

keywords: Desalination, Polyurethane foam, MIL-125, and Evaporation rate

1.Introduction

Freshwater supplies are decreasing because of industry usage and high wastewater discharge (1). Pure water is an important for different uses such as drinking, agriculture and industrial applications (2-4). We should search and solve freshwater source shortages to satisfy the increasing population and energy needs will rise in recent time. Desalination is one of the strategies for producing pure water from contaminated water, salty, or brackish (5). All desalination strategies can be demonstrated to solve the lack of freshwater source. These methods, which can include mechanical vapour compression (MVC), low-temperature desalination (LTD), multi-effect desalination (MED), reverse osmosis (RO), multi-stage flash distillation (MSF), membrane distillation (MD) involve high energy consumption, and high costs (6-8). We can enhance evaporation efficiency and use alternative energy sources for heating in seawater desalination as solar energy (9, 10). The solar steam generation techniques can easily produce heat water from light with small photothermal conversion efficiency (11). Steam is produced using photothermal conversion materials (PCMs) at the water-air interface, where it can provide heat from solar energy and prevent heat loss to the bulk water (12-15). For solar desalination to be very efficient, the photothermal layer must absorb light. We demonstrate other solar absorbers with metal organic frameworks and graphene oxide to increase the rate evaporation.

Metal-organic frameworks (MOFs) are an attractive candidate due to evaporation-driven electricity generation, their charged surface, and hydrophilicity for example MIL125 for water desalination. MIL-125(Ti) exhibited light response properties because of development of new Ti-MIL structures and can be driven by light and transport electrons to the metal center(16-18). MIL-125 has water permeability, high efficiency, and salt rejection in the desalination technique (19-22). Due to its effective light absorption, salt rejection property , electrical, optical, biological uses, graphene oxide (GO), which exhibited a broad spectrum of light absorption from the visible to NIR range, has also been investigated as a

photothermal material for solar desalination (23,24). Herein, we prepare nanostructured MIL125 as solar evaporators and can enhance evaporation performance by modification of MIL-125 by addition of GO. In this paper, we developed a floating polyurethane foam (PU) that is combined with a photothermal composite using a simple technique.

2. Materials and methods

All solvents and chemicals were used without purification. 1,4-benzene dicarboxylic acid (H_2BDC),Titanium (IV) isopropoxide (TTIP), methanol, and N, N-dimethylformamide (DMF) were supplied from Sigma Aldrich. For preparation of GO, the following substances were used as follow: graphite powder (99.95%), sodium nitrate ($NaNO_3$), potassium permanganate ($KMnO_4$), 30% hydrogen peroxide (H_2O_2) , sulfuric acid (H_2SO_4), and Hydrochloric acid (HCl). Graphene oxide was prepared by using graphite flakes by a modified Hummer technique [25]. The solvothermal method was used to prepare MIL-125 depending on these procedures. Mixture of methanol (5 mL) and anhydrous DMF (45 mL) were used to dissolve 1,4 benzene dicarboxylic acid (15 mmol). Subsequently, Titanium (IV) isopropoxide (9 mmol) was added to mixture and stirring for 10 min. The mixture was poured into a Teflon tube , heated at 120 ºC for 16 hours and was placed in a oven. The autoclave was cooled to reach room temperature. Finally, we separated the white of MIL-125 by centrifuge and washed the precipitate several times by DMF and then diluted ethanol. Finally, the white precipitate was dried at 80 ºC.

2.1. Characterization techniques

XRD measurements of samples were recorded by Philips (PW 150) X-ray diffractometer instrument by using Ni-filtered Cu (K_α) radiation with wavelength (λ) = 1.540 A^o at 45 mA and 40 KV. The scanning was made for a two-theta angle from 1 to 60. FT-IR analysis of samples was showed by FT-IR spectroscopic technique on Nicolet Magna-IR 550 spectrometers with 128 scans and 4 cm^{-1} resolution in the mid-IR region 400-4000 cm^{-1}. Each sample was mixed with KBr substance and pressed into a thin wafer that was placed into the IR cell and then the spectrum was recorded. Samples were investigated by the SEM technique to explain the structure morphology. The surface images of samples were showed by JEOL-JSM-6510 LV scanning electron microscope. Samples was put on gold-coated grid and scanned with a focused electrons beam. A Sci-Sun-300 AAA solar simulator was investigated to explain the solar steam generation tests. A thermocouple was used to study thermal absorber surface's temperature during the desalination strategy, and an IR camera could show the surfaces' thermal pictures.

2.2. Synthesis of the photoabsorber materials

Polyurethane foam was used to prepare a one-layer system for solar-driven water desalination. Initially, polyol and liquid diisocyanate were combined with 0.5 g of fabricated composites for 6–8 seconds. After 10 min, the fabricated foam was cut into disks with 4.5 cm diameter and 1 cm thickness and kept for further use. Finally, polyurethane foam can float in 100 mL of saline water.

2.3. Evaporation performance under one sun

The steam generation experiment was carried for pure and saline water under an ambient temperature of 22 °C ± 3 °C and a humidity of 50% for 1 hour. The polyurethane foam with prepared samples was floated in 100 ml beaker with 100 ml DI water or saline water. The mass loss of water in 60 min through evaporation was showed by using an electronic analytical balance (1 mg inaccuracy) every 5 minutes. The temperature distribution of evaporators before and after illumination was measured by an IR camera and thermocouple, respectively. The evaporation rate was calculated using equation (1).

$$v = \frac{dm}{Sdt} \qquad (1)$$

The evaporation rate (v) can be measured by equation (1) (39, 45) that S is the surface area of foam, m is the weight of the evaporated water (Kg), and t is the time of illumination.

3. Results and Discussion

3.1. characterization

Fig. 1b showed the XRD patterns of the pure MIL-125 and GO@MIL-125. The XRD pattern of pure MIL-125, the peaks allocated at 2θ = 6.9°, 9.9°, 11.9°, 15.7°, 18°, 19.2°, 22.8°, 23.7°,

34.3° and 49.3° attached to the (101), (002), (211), (220), (310), (222), (312), (213), (400) crystal planes, respectively (26-29). Fig. 1b showed the GO@ MIL-125 composite has diffraction peaks similar to MIL-125. Small broad band was showed at $2\theta = 26°$ and XRD pattern of GO observed a characteristic peak at 11.9º which small increased after incorporation into MIL structure due to low percentage loading. This result demonstrated that MIL-125 crystals were completely formed with GO sheets (30) .

The functional groups of MIL-125 and GO@MIL-125 were showed by FTIR spectra as investigated in Fig. 1b. The broad adsorption band in 3200-3400 cm^{-1} range was noticed in the FTIR spectra of MIL–125 for free solvent molecules in pores of frameworks (31). The vibration of carboxylate groups caused by the linker in frameworks produced the bands at 1291-1690 cm-1 (32). The bands at 500-800 cm-1 belonged to Ti-O-C and Ti-O-Ti vibrations, whereas the bands in the 800-1200 cm-1 range were the characteristic absorption band of the benzene ring (33). The transmittance of bands increased by increasing the GO concentration loaded on MIL-125The absorption band at 1600 cm^{-1} due to Ti−O−C bonds and interactions between MIL-125 and GO nanosheets increased. A new absorption band allocated around 1000 cm^{-1} as the π−π interaction between frameworks and GO sheets. The absorption band at 620 cm^{-1} of the Ti-O-Ti stretching vibration was weakened in GO@MIL-125. This proved that there may exist some interaction between MIL-125 and GO(34).

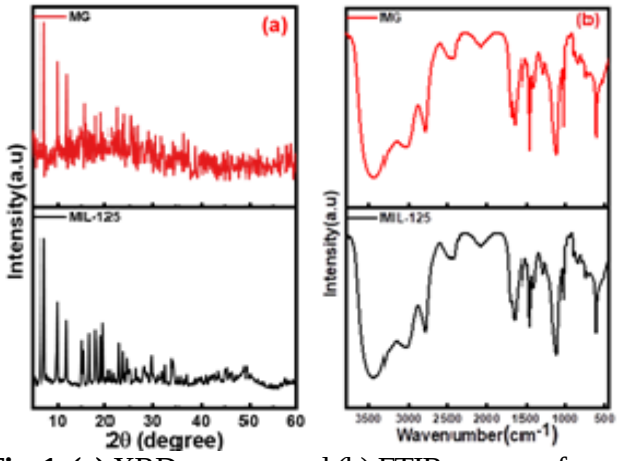

Fig. 1. (a) XRD patterns and (b) FTIR spectra of MIL-125 and GO@ MIL-125.

The morphology of GO@MIL-125 on PU foam was showed by using SEM analysis. Fig. 2 displayed the structural properties of GO@MIL-125 as investigated by SEM. The porosity property of the fabricated polyurethane foam was noticed in the SEM images which include the hydrophilic nature and the open porous of the fabricated Polyurethane foam. SEM images showed MIL-125 features a spherical shape with a smooth surface and GO with sheet in shape (35-37).

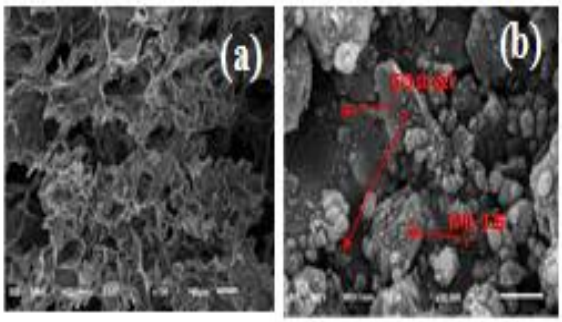

Fig 3. SEM images of (a) PU foam, and (b) MG composite

3.2. Solar steam generation process

To show the steam generation performance for two foams were prepared by M, and MG. The performance of photo thermal absorbers was proved by the solar simulator utilizing polyurethane foam in 1 sun for 1 hour for the solar steam generation performance. Each sample was combined with foam with 4.5 cm diameter. The foam was wetted with deionized water before being placed on the surface of the 100 mL of water in the beaker. Using an electronic balance, the mass loss was estimated, and the evaporation rate was calculated from the mass loss calculated at 5 min up to 1h. Fig .3a showed the mass loss of two pure water photothermal absorbers throughout the steam generation test. The results showed that pure foam has the smallest mass loss of water of 0.31 kg m^{-2} in all samples because pure PU foam has a small thermal absorptivity but also increased the light absorption by its modification of foam (38). The mass loss of water by using M and MG absorbers were 0.44 and 0.62 kg m^{-2}. Large surface-active sites and photosensitive characteristics of MIL-125 contributed to water permeability and salt rejection during the desalination process (39). The solar absorbers including GO enhanced the rate of evaporation due to low reflectance, and low thermal conductivity GO (40, 41). The carboxylic and hydroxyl functional groups in graphene oxide structure are necessary for increasing the evaporating rate of water due to the strong π–π

interactions between the MOF and GO which can increase the electron−hole pair separation. The results of photothermal foams in artificial saline water for PU, M, and MG evaporators were shown in Fig. 3b. The mass loss of absorbers was 0.19, 0.35, and 0.54 kg m^{-2} in saline water. The results in saline water were lower than pure water due to the presence of salt ions. The mass loss decreased by increasing salt in the solution because salt on the foam's surface had precipitated, it blocked incident light and decreased water evaporation.

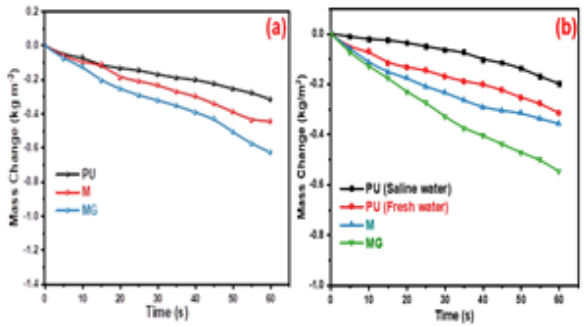

Fig.3. (a) mass changes for PU, M, and MG (b) mass change for PU, M, and MG of pure and saline water

Solar steam generation for fabricated photothermal evaporators; M, and MG The temperature change of two solar absorbers after 1 sun irradiation for 1h was compared in Fig. 4a. The temperature on surface of foams enhanced from room temperature to 30.6, and 34.3^{0}C for M and MG respectively. The MG temperature was larger than M due to high solar absorption and hydrophilic surface property because of combination between MIL-125 and GO together. After illumination for 1h, the temperature changes on poly urethane foams surface were recorded by IR camera and thermocouple as showed in Fig. 4b.

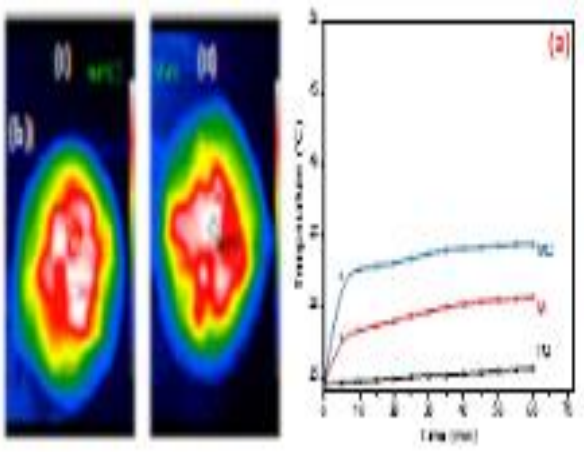

Fig. 4 (a) Temperature change on polyurethane foams surface in 60 min and (b) IR thermal images of (I) M, and (II) MG after 1h.

4.Conclusion

In summary, for solar water desalination, we fabricated a one layer system of graphene oxide supported MIL-125 with polyurethane foam (MGPU). PU was an important for self-floating, low thermal conductivity, and high absorption of light. MIL-125 has water permeability and salt rejection in the desalination technique. we can improve MIL-125 foam by using GO to enhance the evaporation rate of water attached to the physical characteristics of MIL-125 and graphene oxide in desalination technique. The fabricated samples can produce clean condensed freshwater in solar water desalination technique.

5.References

1. Xu Y, Ma J, Liu D, Xu H, Cui F, Wang W. Origami (2019) system for efficient solar driven distillation in emergency water supply. *Chemical Engineering Journal*.;356:869-**76**.
2. Mekonnen MM, Hoekstra AY. Four (2016)billion people facing severe water scarcity. ScienceAdvances.:1-6.
3. Nayi KH, Modi KV. (2018) Pyramid solar still: A comprehensive review. Renewable and Sustainable Energy Reviews.;**81**:136-48.
4. Fang Z, Zhen YR, Neumann O, Polman A, Garcia de Abajo FJ, Nordlander P, et al. (2013) Evolution of light-induced vapor generation at a liquid-immersed metallic nanoparticle. Nano Lett.;**13(4):**1736-42.
5. Ramalingam K, Liang M, Pyae NLW, Aung SH, Oo TZ, Srimuk P, et al. (2020) Self-Sustained Visible-Light-Driven Electrochemical Redox Desalination. ACS Appl Mater Interfaces.;**12(29):**32788-96.
6. Lv J, Chen Z-L, Tang J, Chen L, Xie W-J, Sun M-X, et al. (2022); Study on the superhydrophilic modification and enhanced corrosion resistance method of aluminum alloy distillation desalination tubes. Surface and Coatings Technology. 446.
7. Srimuk P, Su X, Yoon J, Aurbach D, Presser V. Charge(2020)-transfer materials for electrochemical water desalination, ion separation and the

recovery of elements. Nature Reviews Materials.;**5(7):**517-38.
8. Suss ME, Presser V. Water (2018);Desalination with Energy Storage Electrode Materials. Joule. **2(1):**10-5.
9. Alduraibi M, Hezam M, Al-Ruhaimi B, El-Toni AM, Algarni A, Abdel-Rahman M, et al. (2020)Rapid Room-Temperature Synthesis of Mesoporous TiO(2) Sub-Microspheres and Their Enhanced Light Harvesting in Dye-Sensitized Solar Cells. Nanomaterials (Basel).;**10(3).**
10. Wang M, Zhang J, Wang P, Li C, Xu X, Jin Y. Bifunctional(2018) plasmonic colloidosome/graphene oxide-based floating membranes for recyclable high-efficiency solar-driven clean water generation. Nano Research.;**11(7):**3854-63.
11. Tao P, Ni G, Song C, Shang W, Wu J, Zhu J, et al. (2018)Solar-driven interfacial evaporation. Nature Energy.;**3(12):**1031-41.
12. Weng D, Xu F, Li X, Li Y, Sun J. (2018)Bioinspired photothermal conversion coatings with self-healing superhydrophobicity for efficient solar steam generation. *Journal of Materials Chemistry A.*;**6(47):**24441-51.
13. Sun L, Liu J, Zhao Y, Xu J, Li Y. (2019) Highly efficient solar steam generation via mass-produced carbon nanosheet frameworks. Carbon.;145:352-**8**.
14. Gao M, Zhu L, Peh CK, Ho GW. Solar (2019)absorber material and system designs for photothermal water vaporization towards clean water and energy production. Energy & Environmental Science.;**12(3):**841-64.
15. Zhao F, Zhou X, Shi Y, Qian X, Alexander M, Zhao X, et al. (2018) Highly efficient solar vapour generation via hierarchically nanostructured gels. Nat Nanotechnol.;**13(6):**489-95.
16. Isaka Y, Kondo Y, Kawase Y, Kuwahara Y, Mori K, Yamashita H. Photocatalytic (2018);production of hydrogen peroxide through selective two-electron reduction of dioxygen utilizing amine-functionalized MIL-125 deposited with nickel oxide nanoparticles. Chem Commun (Camb). **54(67):**9270-3.
17. Zhan W, Sun L, Han X. (2019) Recent Progress on Engineering Highly Efficient Porous Semiconductor Photocatalysts Derived from Metal-Organic Frameworks. Nanomicro Lett.;**11(1)**:1.
18. Zhao SN, Wang G, Poelman D, Van Der Voort P. (2018)Metal Organic Frameworks Based Materials for Heterogeneous Photocatalysis. Molecules.;**23(11).**
19. Dhakshinamoorthy A, Li Z, Garcia H. (2018)Catalysis and photocatalysis by metal organic frameworks. Chem Soc Rev.;**47(22):**8134-72.
20. Zhu J, Li P-Z, Guo W, Zhao Y, Zou R. (2018)Titanium-based metal–organic frameworks for photocatalytic applications. Coordination Chemistry Reviews.;359:80-101.
21. Yang H, Zhao M, Zhang J, Ma J, Wu P, Liu W, et al. (2019) A noble-metal-free photocatalyst system obtained using BODIPY-based MOFs for highly efficient visible-light-driven H2 evolution. *Journal of Materials Chemistry A.*;**7(36):**20742-9.
22. Tahir M, Tahir B, Amin NAS, Muhammad A. (2016) Photocatalytic CO2 methanation over NiO/In2O3 promoted TiO2 nanocatalysts using H2O and/or H2 reductants. Energy Conversion and Management.;119:368-**78**.
23. Han X, Zang L, Zhang S, Dou T, Li L, Yang J, et al. (2020); Hydrophilic polymer-stabilized porous composite membrane for water evaporation and solar desalination. RSC Adv. **10(5):**2507-12.
24. Shen C, Zhu Y, Xiao X, Xu X, Chen X, Xu G. (2020) Economical Salt-Resistant Superhydrophobic Photothermal Membrane for Highly Efficient and Stable Solar Desalination. ACS Appl Mater Interfaces.;**12(31):**35142-51.
25. Néstor ML , Francisco PR and Carlos GG, (2022) Eco-Friendly Approach for Graphene Oxide Synthesis by Modified Hummers Method. Materials., 15, 7228.
26 Olowoyo JO, Saini U, Kumar M, Valdés H, Singh H, Omorogie MO, et al. (2020)Reduced graphene oxide/NH2-MIL-125(Ti) composite: Selective CO2 photoreduction to methanol under visible light and computational insights into

charge separation. *Journal of CO2 Utilization*.;42.
27 Li Z, Che G, Jiang W, Liu L, Wang H. (2019)Visible-light-driven CQDs@MIL-125(Ti) nanocomposite photocatalyst with enhanced photocatalytic activity for the degradation of tetracycline. RSC Adv.;**9(57):**33238-45.
28 Rahmani A, Emrooz HBM, Abedi S, Morsali A. (2018)Synthesis and characterization of CdS/MIL-125 (Ti) as a photocatalyst for water splitting. Materials Science in Semiconductor Processing.;**80:**44-51.
29 Bakbolat B, Daulbayev C, Sultanov F, Beissenov R, Umirzakov A, Mereke A, et al. (2020) Recent Developments of TiO(2)-Based Photocatalysis in the Hydrogen Evolution and Photodegradation: A Review. Nanomaterials (Basel).;**10(9).**
30. W. Li, H. Zhang, T. Chen, L. Yang, C. Sheng, H. Wu, N. (2021)Mao, Robust self-cleaning effects of cotton fabrics coated with reduced graphene oxide (RGO)-titanium dioxide (TiO2) nanocomposites, *Textile Research Journal*, **92** 739-759.
31. Yang Z, Xu X, Liang X, Lei C, Cui Y, Wu W, et al. (2017) Construction of heterostructured MIL-125/Ag/g-C3N4 nanocomposite as an efficient bifunctional visible light photocatalyst for the organic oxidation and reduction reactions. Applied Catalysis B: Environmental.;205:42-54.
32. Yang Z, Ding J, Feng J, He C, Li Y, Tong X, et al. (2018) Preparation of BiVO4/MIL-125(Ti) composite with enhanced visible-light photocatalytic activity for dye degradation. Applied Organometallic Chemistry.;**32(4).**
33. Dargahi Z, Asgharzadeh H, Maleki-Ghaleh H. (2018);Synthesis of Mo-doped TiO2/reduced graphene oxide nanocomposite for photoelectrocatalytic applications. Ceramics International. **44(11):**13015-23.
34. Singaram B, Jeyaram J, Rajendran R, Arumugam P, Varadharajan K. (2018) Visible light photocatalytic activity of tungsten and fluorine codoped TiO2 nanoparticle for an efficient dye degradation. Ionics.;**25(2):**773-84.
35. Awad FS, Kiriarachchi HD, AbouZeid KM, Özgür Ü, El-Shall MS. (2018) Plasmonic Graphene Polyurethane Nanocomposites for Efficient Solar Water Desalination. ACS Applied Energy Materials.;**1(3)**:976-85.
36. Zhang Y, Yan H, Wang X, Zhang Z, Liu F, Tu S, et al(2022). Highly efficient solar-absorber composite material based on tetrapyridylporphyrin for water evaporation and thermoelectric power generation. RSC Adv.;**12(45):**28997-9002.
37. Chen G, Sun J, Peng Q, Sun Q, Wang G, Cai Y, et al. (2020) Biradical-Featured Stable Organic-Small-Molecule Photothermal Materials for Highly Efficient Solar-Driven Water Evaporation. Adv Mater.;**32(29):**e1908537.
38. Kospa DA, Ahmed AI, Samra SE, Ibrahim AA. (2021); High efficiency solar desalination and dye retention of plasmonic/reduced graphene oxide based copper oxide nanocomposites. RSC Adv. **11(25):**15184-94.
39. Fang Y, Ma Y, Zheng M, Yang P, Asiri AM, Wang X. (2018)Metal–organic frameworks for solar energy conversion by photoredox catalysis. Coordination Chemistry Reviews.;373:83-115.
40. Li R, Zhang W, Zhou K. (2018) Metal-Organic-Framework-Based Catalysts for Photoreduction of CO(2). Adv Mater.;**30(35):**e1705512.
41. Shao B, Wu X, Wang Y, Gao T, Liu Z-Q, Owens G, et al. (2020) A general method for selectively coating photothermal materials on 3D porous substrate surfaces towards cost-effective and highly efficient solar steam generation. *Journal of Materials Chemistry A*.;**8(46):**24703-9.